Available online at www.sciencedirect.com
SCIENCE DIRECT®
C. R. Palevol 5 (2006) 35–43
COMPTES RENDUS PALEVOL
http://france.elsevier.com/direct/PALEVO/

Human Palaeontology and Prehistory

Climate and hydrological changes in tropical Africa during the past million years

Françoise Gasse

CEREGE, UMR 6635, BP 80, 13545 Aix-en-Provence cedex 04, France

Received 21 February 2005; accepted after revision 19 September 2005
Available online 22 November 2005
Written on invitation of the Editorial Board

Abstract

Tropical African climate has oscillated between markedly wetter and drier conditions on all timescales in response to global climate disturbances. A step-like increase in aridity over the past 3 Ma has been primarily paced by orbital cycles coupled with the onset and amplification of high-latitude glacial cycles. On the 10^4–10^3-ka timescales, observed changes imply interactions between insolation, sea-surface conditions and vegetation. High-frequency variations could be linked to oscillations in major atmospheric circulation modes, in solar output, or to major volcanic events. ***To cite this article: F. Gasse, C. R. Palevol 5 (2006)***.

Résumé

Changements climatiques et hydrologiques en Afrique tropicale au cours des derniers millions d'années. Le climat d'Afrique tropicale a connu une alternance de périodes humides et sèches, en réponse à des changements du climat global, à toutes échelles de temps. Un accroissement par étapes de l'aridité depuis 3 Ma traduit le forçage astronomique et la mise en place des cycles glaciaires des hautes latitudes. Aux échelles 10^4–10^3 ka, les changements observés impliquent des interactions entre facteurs orbitaux, conditions de surface des océans, et végétation. Les variations à haute fréquence seraient associées à des oscillations des grands modes de circulation atmosphérique, de l'activité solaire, ou à des événements volcaniques majeurs. ***Pour citer cet article : F. Gasse, C. R. Palevol 5 (2006)***.

Keywords: Tropical Africa; Palaeoclimates; Palaeohydrology; Pliocene; Quaternary

Mots clés : Afrique tropicale ; Paléoclimats ; Paléohydrologie ; Pliocène ; Quaternaire

Version française abrégée

Introduction

Depuis 4 millions d'années (Ma), le climat de l'Afrique tropicale a oscillé entre périodes humides et sèches, de l'échelle de temps interannuelle à l'échelle du million d'années (Fig. 1). La revue présentée ici, qui s'appuie sur un bon nombre d'ouvrages de synthèse, se propose d'illustrer comment ces variations climatiques sont reliées à la variabilité du climat global.

Principaux traits du climat d'Afrique actuel

La zonalité marquée du climat reflète la distribution des champs de pression et les vents dominants à basse

E-mail address: gasse@cerege.fr (F. Gasse).

1631-0683/$ - see front matter © 2005 Académie des sciences. Published by Elsevier SAS. All rights reserved.
doi:10.1016/j.crpv.2005.09.012

altitude. Les déserts du Sahara et de Namibie sont dominés par les anticyclones subtropicaux. Une large ceinture de climat tropical sépare ces déserts. Les migrations saisonnières de la zone de convergence intertropicale (ITCZ) (Fig. 2) résultent en une zone de climat équatorial à deux saisons des pluies, flanquées au nord et au sud par de larges bandes de climat de mousson, avec une saison des pluies estivale et un hiver sec.

La zonalité du climat est altérée par les conditions de surface océaniques, telles que les courants, ou les anomalies de température engendrées par exemple par le mécanisme *El Niño Southern Oscillation* (ENSO), dont les réponses sur le continent diffèrent selon les régions [30]. La topographie, en particulier les hauts reliefs d'Afrique de l'Est, est aussi responsable des différences climatiques régionales.

Changements du climat d'Afrique tropicale à l'échelle astronomique

Les enregistrements paléoenvironnementaux montrent un accroissement de l'aridité depuis environ 3 Ma, ponctués par des intervalles d'amplification du phénomène, synchrones des étapes de mise en place et d'amplification des cycles glaciaires des hautes latitudes.

En Afrique de l'Est, les données palynologiques mettent en évidence des refroidissements marqués vers 3,3 Ma et 2,5 Ma [5,6]. D'après l'étude des faunes de mammifères du bassin de l'Omo [4], les espèces de forêts et savanes boisées sont relayées par des espèces de prairies entre 3,6 et 2,4 Ma, avec une étape d'accentuation vers 2,6–2,4 Ma (Fig. 3A). L'analyse isotopique des carbonates des sols des bassins de Turkana et d'Olduvai démontre le remplacement des forêts par des savanes herbacées ouvertes entre 3 et 1 Ma, par étapes marquées vers 1,8, 1,2 et 0,8 Ma [9,10] (Fig. 3B). Les sédiments lacustres et leur flore de diatomées témoignent de l'existence de grands lacs permanents et de conditions très humides jusque vers 0,8 Ma, par exemple en Afar [14] (Fig. 3C) et dans le rift kenyan [3].

Les séquences marines continues prélevées au large de l'Afrique de l'Est et de l'Ouest renseignent sur les conditions climatiques du continent. Ainsi, les flux de poussières éoliennes – indicateurs d'aridité et de la force des vents – s'accroissent de façon continue depuis 3 Ma, avec des phases d'augmentation rapide vers 2,8, 1,7 et 1,0 Ma [13] (Fig. 3D). Parallèlement, les périodicités de la variabilité éolienne changent : au cycle de précession orbitale (23–19 ka), principal facteur contrôlant la variabilité de la mousson durant tout le Néogène, se surimposent les cycles glaciaires des hautes latitudes : 41 ka après 1,8–1,6 Ma ; 100 ka après 1,2–0,8 Ma [13] (Fig. 3E).

Le forçage astronomique a joué un rôle prépondérant. Le couplage pôles froids–tropiques secs est en bon accord avec les simulations des modèles de circulation générale (GCMs) [8].

Interactions entre les composants du système climatique à l'échelle multimillénaire

Du fait de la géométrie de la précession orbitale, les changements d'insolation d'été sont en antiphase entre les deux hémisphères (Fig. 4A) [2]. Le forçage orbital prédit des conditions sèches sur les tropiques nord et un renforcement des pluies sur les tropiques sud pendant le dernier maximum glaciaire (LGM ; ~23–19 ka BP), et une réponse inverse pendant l'Holocène inférieur et moyen (EMH, ~11,5–5 ka BP) [2,7,8].

Les données sur les tropiques nord paraissent en bon accord avec les fluctuations d'insolation d'été, mais plusieurs enregistrements suggèrent des conditions plus sèches qu'aujourd'hui dans les tropiques sud pendant le LGM [1,15] (Fig. 4). Cette aridité est principalement attribuée à l'abaissement des températures de surface océanique (SSTs) au LGM. Une diminution des précipitations d'été sur la plus grande partie des zones tropicales est en accord avec les simulations des GCMs [8,25].

Une manifestation spectaculaire du changement climatique est la mise en place d'un Sahara humide et vert pendant le EMH. Les données indiquent une migration vers le nord des ceintures de précipitation tropicale de 5–10°. Toutes les simulations de GCMs montrent un renforcement du flux de mousson en réponse à l'augmentation d'insolation d'été, mais la meilleure cohérence avec les données s'observent avec les modèles couplés atmosphère–océan–végétation [7,8,12].

Changements climatiques rapides

De sévères événements climatiques recensés en Afrique aux échelles de temps inférieures à 1000 ans [15–18,30,31] sont souvent associés à des déséquilibres du système climatique affectant de larges régions du globe.

Ainsi, un intervalle très sec interrompt la grande période humide du EMH des tropiques nord vers 9–8 ka BP [15–18] (Figs. 1C et 4B–C). Il est associé à un affaiblissement de la mousson d'été en mer d'Arabie et au Tibet [18,23] et à un intervalle froid dans l'hémisphère nord [23]. Les causes de cet événement global sont encore débattues [23]. Deux enregistrements

paléoclimatiques, l'un en Afrique du Sud (Makapansgat), l'autre au Kenya (Naivasha, Fig. 1B) [31] s'avèrent en antiphase sur presque tout le dernier millénaire [30]. Aujourd'hui, les anomalies de précipitations associées à l'ENSO sont inversement corrélées entre ces deux régions [30]. Il est vraisemblable que des changements à basse fréquence du mode de circulation ENSO, soient responsables des différences régionales observées à l'échelle multi-décennale à centennale.

Conclusions

Quelle que soit l'échelle de temps, les oscillations humides/arides recensées en Afrique tropicale au cours du Plio-Quaternaire paraissent associées à de profonds changements du système climatique global ou à la dynamique régionale des échanges atmosphère–océan–biosphère.

1. Introduction

During the last 4 millions of years (Ma), tropical African climate has oscillated between markedly wetter and drier conditions. These changes have occurred on all timescales (Fig. 1). In recent times, catastrophic rainfall events in equatorial East Africa, the drastic Sahel drought in the 1970–1980s, or rapid lake-level fluctuations have illustrated the large interannual-decadal rainfall variability (Fig. 1A) and its serious impact on societies. But changes of much larger magnitude and duration have occurred in the past. On the interdecadal–centennial timescale (Fig. 1B), well-dated records combining geological, documentary and archaeological data suggest strong links between floods/droughts and changes in civilisation [30,31]. From ~11.5–5.5 ka BP ago (ka BP means 10^3 calendar years before present), East African Rift lakes extended tens or even hundreds of metres above their present-day level (Fig. 1C), while Neolithic civilisations flourished in a wet and green Sahara [15,16]. On timescales of 10^4–10^6 yr, geological and palaeobiological data document an alternation of wet and dry episodes (Fig. 1D) [29], and a step-like increase in aridity since ~3 Ma (Fig. 1E) [9,10,13]. High-amplitude climate changes have induced biome shifts, species migrations, community reorganisation, and changes in water resources of considerable importance for human populations.

The abundant literature on climate changes in Africa cannot be included here. This paper refers to several synthesis works where the reader will find original references and detailed discussions. After a brief overview of modern climates, the paper aims to illustrate

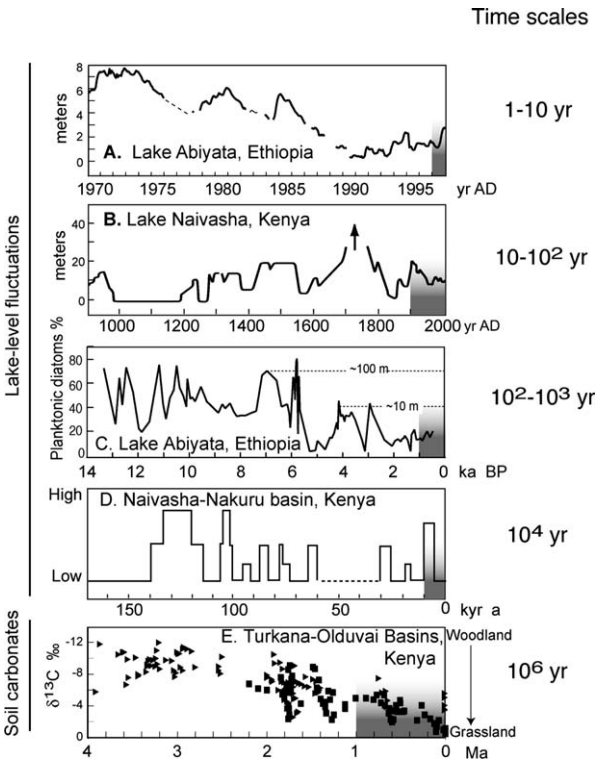

Fig. 1. Examples of hydrological fluctuations in tropical Africa on different timescales. Instrumental (**A**) and reconstructed (**B**–**D**) lake-level fluctuations, after **A**: [21]; **B**: [31]; **C**: [11,18]. **E**: Isotope record of soil carbonates, indicator of palaeovegetation, after [9,10]. See Fig. 2 for site location.

Fig. 1. Exemples de fluctuations hydrologiques en Afrique tropicale à différentes échelles de temps. Fluctuations de niveaux lacustres mesurées (A) et reconstruites (B–D), d'après **A** : [21] ; **B** : [31] ; **C** : [11,18]. **E** : Enregistrement isotopique des carbonates de sols, indicateur de la paléovégétation, d'après [9,10]. Voir la Fig. 2 pour la localisation des sites.

how Plio-Quaternary climate changes in Africa are linked to global climate variability, from long-term oscillations, to high-frequency fluctuations that took place at the timescale of human lives.

2. Major modern climatic features of Africa

African climates depend primarily on low altitude pressure and winds over the continent. The northern and southern ends of the continent experience extra-tropical (Mediterranean) climates. They are both flanked by deserts (Sahara and Namib deserts), dominated by the subtropical anticyclones. A wide belt of tropical climates separates the two arid zones. A zone of maximum rainfall related to the Intertropical Convergence Zone (ITCZ) follows the overhead position of the sun. The seasonal ITCZ migration (Fig. 2) results in an equatorial zone of

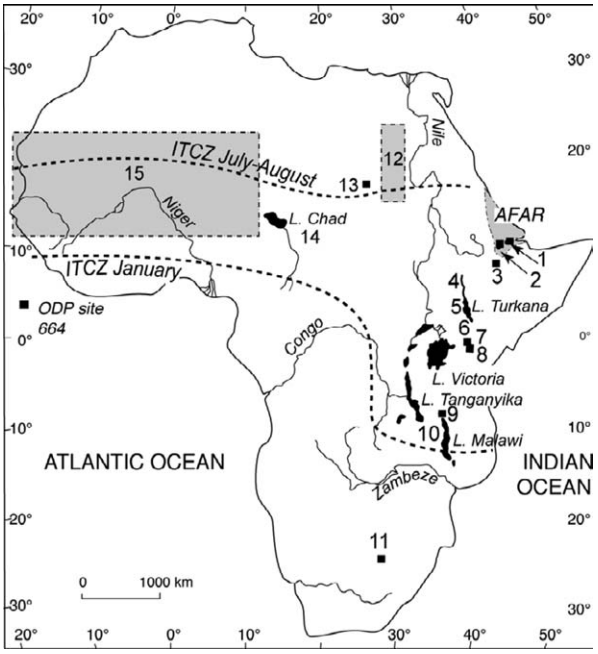

Fig. 2. Map of Africa showing the ITCZ position in boreal and austral summers, and location of sites or regions called in text and figures. **1**: Central Afar, L. Abhé; **2**: southern Afar, Middle Awash Valley (Hadar, Bodo); **3**: L. Abiyata; **4**: Omo R.; **5**: Turkana basin; **6**: Olduvai; **7**: Nakuru-Elmenteita basin; **8**: L. Naivasha; **9**: L. Massoko; **10**: L. Malawi; **11**: Makapansgat Valley; **12**: eastern Sahara Holocene pollen sites used in Fig. 5; **13**: West Nubian palaeolake; **14**: Chad basin; **15**: western Sahara–Sahel Holocene pollen sites used in Fig. 5.
Fig. 2. Carte d'Afrique montrant la position de l'ITCZ en été boréal et en été austral, et localisation des sites ou des régions appelées dans le texte et les figures. **1** : Afar central, L. Abhé ; **2** : Afar méridional, moyenne vallée de l'Awash (Hadar, Bodo) ; **3** : L. Abiyata ; **4**. rivière Omo ; **5** : bassin de Turkana ; **6** : Olduvai ; **7** : bassin de Nakuru-Elmenteita ; **8** : L. Naivasha ; **9** : L. Massoko ; **10** : L. Malawi ; **11** : vallée de Makapansgat ; **12** : sites palynologiques holocènes du Sahara oriental, utilisés sur la Fig. 5 ; **13** : paléolac Ouest-Nubien ; **14** : bassin du Tchad ; **15** : sites palynologiques holocènes du Sahara–Sahel occidental, utilisés sur la Fig. 5.

humid climates with two seasonal rainfall maximum, flanked on the north and south by broad belts of monsoonal climates with a single summer rainy season and winter drought. The West African monsoon is driven by the pressure gradient that develops during the boreal summer between the high-pressure system over the subtropical southern Atlantic Ocean and the heated land-surface of the Sahara-Sahel; it penetrates far inland over northeastern Africa. The East African monsoon system shows reversed sub-meridional flows originating from the subtropical high cells over the southern Indian Ocean and over Arabia during the northern and southern hemisphere summer, respectively.

The zonal climate pattern is altered by sea-surface conditions. For example, the cold Benguela, and the warm Algulhas currents flowing along the western and eastern coasts of southern Africa, respectively, contribute to the east–west climate asymmetry. Interannual rainfall fluctuations in many areas of the continent are statistically linked to the El Niño Southern Oscillation (ENSO), or with sea-surface temperature (SSTs) fluctuations in the Indian and Atlantic Oceans which often occur in the context of ENSO. The sign of the ENSO-related rainfall anomalies differ, however, with the regions [30].

Regional climates also depend on orography. For example, highland areas in East Africa generate marked climatic gradients over short distances. Mountains receive high rainfall, while the basins of the East African Rift lie in the rain shadow of their bordering escarpments and are semi-arid. This topography results from the geological history of the continent at timescales longer than 10^6 yr. Tectonics and volcanism, still active in the East African Rift system, have induced significant changes in the regional water balances during the Late Neogene. The great East African lakes also play a role on regional climate through water recycling.

3. African climate changes on the orbital timescale

Well-dated terrestrial and marine African records document an overall increase in aridity since 3–2.8 Ma with step-like shifts at 2.8–2.4, 1.8–1.6, and 1.2–0.8 Ma. These shifts were synchronous with shifts in the onset and amplification of ice sheet growth and cooling at high latitudes, suggesting coupling between low- and high-latitude climates [13].

No continuous continental record covering the whole Plio-Pleistocene period is available yet. However, palaeovegetation, fossil mammals, and palaeolake records provide information on past African climates with high spatial resolution. East Africa is relatively well known because of its richness in fossil records, including hominids, and radiometric chronologies based on volcanic material bounding the sedimentary sequences. At the hominid-bearing site of Hadar (Middle Awash valley, southern Afar), pollen spectra and biome reconstructions indicate a cooling of ~5 °C and a 200–300 mm yr^{-1} rainfall increase just before 3.3 Ma, consistent with an initial marine $\delta^{18}O$ shift reflecting an increase in global ice volume [5]. Pollen data from various regions of northeastern Africa show regional shifts to cooler and drier vegetation type after ca. 2.5 Myr [6]. A comprehensive examination of the fossil mammal fauna in the Omo basin documents a remarkable decrease in closed woodland and forest species and an increase in grassland species between 3.6 and 2.4 Ma,

with a marked rise between 2.6 and 2.4 Ma [4] (Fig. 3A). Stable isotopic analysis of pedogenic carbonates from the Turkana and Olduvai basins indicate gradual replacement of woodland by open savannah grasslands between 3 and 1 Myr, with step-like increases in savannah vegetation near 1.8, 1.2 and 0.6 Ma (Fig. 3B) [9,10]. Tectonic basins have experienced prolonged intervals of continuous lacustrine sedimentation. In southern Afar, the Bodo and Hadar palaeolakes (ca. 4.0–2.95 Ma) have stored thick sedimentary series where clays, sands, diatomaceous clays and diatomites indicate alternating swamp, shallow saline to freshwater lake environments [13]. Sedimentary bedding cycles were about 20–25 kyr in duration, suggesting that environmental fluctuations are paced by the precessional orbital cycle (in [13]). In central Afar, lacustrine deposits sandwiched between volcanic flows are dated between >2.3 and 0.8 Ma (Fig. 3C) [14]. Large, deep lake environments are represented by 4- to 8-m-thick interbeds of pure, white diatomite characterised by the dominance of large freshwater planktonic species, e.g., *Stephanodiscus niagarae* now living in the North American great lakes. Similar facies and diatom assemblages were found in a 40-m-thick profile that accumulated in a lake at least 100-m deep in the Nakuru-Elmenteita basin, between 1 and ~0.95 Ma [3]. These typical facies and microflora, indicators of a precipitation–evaporation balance (P–E) much higher than today, disappeared forever from Africa by the Middle Pleistocene; further lacustrine phases bear diatom flora found in modern East African lakes and reflect higher evaporation rates [14].

Continuous marine sediment sequences off the western and eastern margins of subtropical Africa have provided evidence for an increase in aridity and greater climate variability in northern Africa after ~3–2.8 Ma through their pollen spectra, clay mineral assemblages, and aeolian dust concentration ([13] and references therein). For example, the study of aeolian dust export from West and East subtropical Africa – a good indicator of continental aridity and trade-wind strength – documents step-like shifts in the amplitude and periods of aeolian variability at ~2.8, 1.7, and 1.0 Ma [13]. It shows that the orbital precession cycle (23–19 ka) was

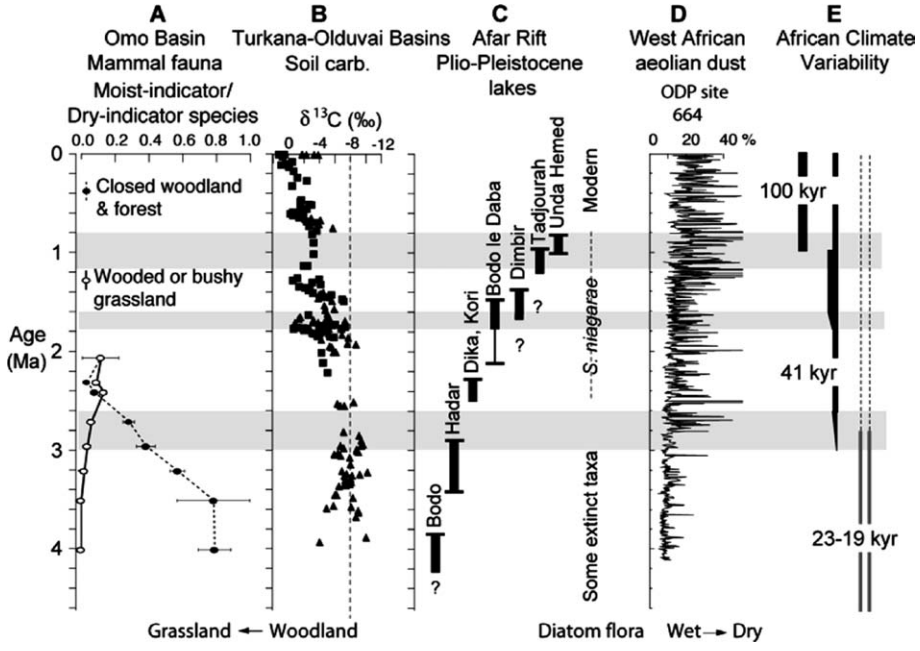

Fig. 3. Some records of African climate variability at the orbital time-scale. **A**–**C**: Terrestrial records. **A** after [4]; **B** after [9,10]; **C** after [6,14]. **D**–**E**: Marine records, after [13]. **D** is an example of aeolian dust record off West Africa, which depends on the vegetation cover and strength of the northeastern trade winds over northwestern Africa. **E** shows the dominant periods found in several dust records off West and East Africa. See Fig. 2 for site location.

Fig. 3. Quelques enregistrements de la variabilité climatique en Afrique, à l'échelle de temps orbitale. **A**–**C** : enregistrements continentaux. **A** d'après [4] ; **B** d'après [9,10] ; **C** d'après [6,14]. **D**–**E** : Enregistrements marins, d'après [13]. **D** représente les flux de poussières éoliennes en un site au large de l'Afrique de l'Ouest, qui dépendent du couvert végétal et de la force des alizés du nord-est sur le Nord-Ouest de l'Afrique. **E** illustre les principales périodes observées dans plusieurs enregistrements de poussières éoliennes au large de l'Afrique de l'Ouest et de l'Afrique de l'Est. Voir la Fig. 2 pour la localisation des sites.

the fundamental driver of African monsoon climate throughout the Late Neogene, but high-latitude glacial cycles of 41 ka after ~1.8–1.6 Ma, and of 100 ka after ~1.2–0.8 Ma were superimposed on the precession signal after 2.8 Ma (Fig. 3D–E) [13].

African climate is thus very sensitive to high-latitude glacial conditions and has been primarily paced by earth orbital variations over the past million years. This is in good agreement with general circulation model (GCM) experiments which show cooler, drier African conditions during the glacial maximum [8].

4. Interactions between the components of the climate system at the multi-millennial timescale

Two time intervals are selected to illustrate interactions between orbital forcing and regional ocean–atmosphere–biosphere dynamics acting on the monsoon system during glacial (the Last Glacial Maximum, LGM, ~23–19 ka BP), and interglacial (the Early–Middle Holocene, EMH, ~11.5–5 ka BP) periods.

Due to the geometry of orbital precession, changes in summer insolation are in antiphase between hemispheres (Fig. 4A) [2]. Increased summer insolation should result in reinforced monsoon circulation by enhancing the inter-hemispheric ocean–land pressure contrast that draws the monsoon winds inland [7,8]. Orbital forcing predicts dry climates in the northern tropics, and enhanced monsoon rainfall in the southern hemisphere during the LGM, and an opposite response during the EMH.

Palaeoclimatic data in the northern tropics roughly follows summer insolation fluctuations [15], but a rainfall deficit also occurred in the southern tropics during the LGM, indicating that the hydrological budget has not only been paced by orbital cycles in glacial times [1,15] (Fig. 4). For example, decreases in P–E are suggested by an increase in diatom-inferred conductivity in Lake Massoko (Fig. 4D) – a small crater lake without surface outlet – around 20 ka BP, and by the high percentages of littoral diatoms by ~23–16 ka BP in the large Lake Malawi. Aridity in tropical Africa under LGM boundary conditions is primarily attributed to lower tropical SSTs, due to increased northward ocea-

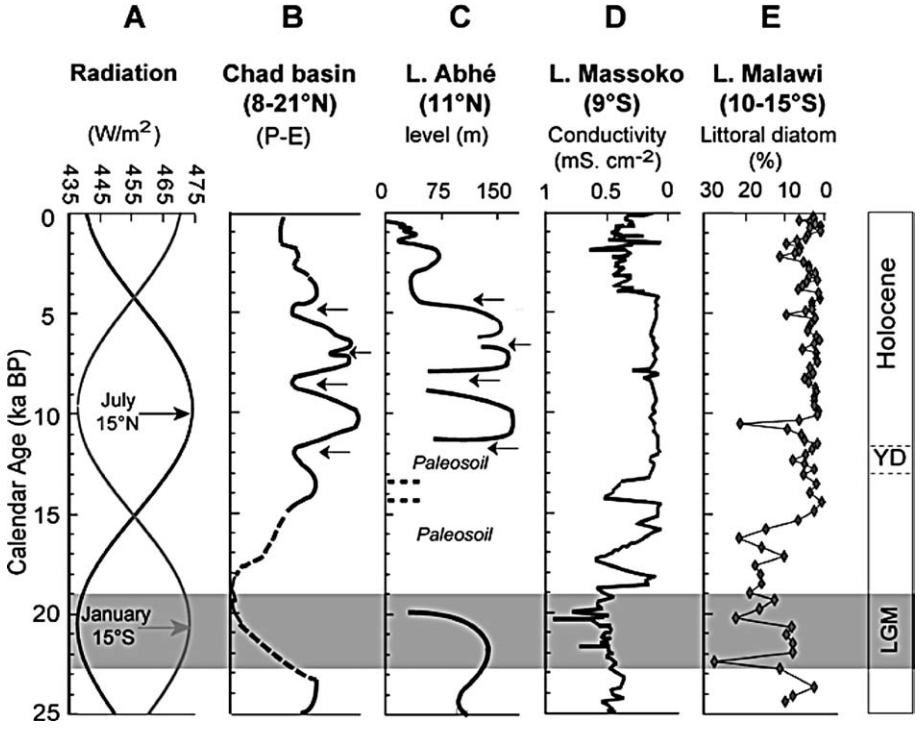

Fig. 4. Relationships between solar radiation and water balance of some lake basins from the northern and southern tropics over the past 25 ka BP. **A**: Summer solar radiation [2]; **B** after [27]; **C** after [15], **D**–**E** after [1]. **LGM**: Late Glacial Maximum; **YD**: Younger Dryas; arrows in **C** and **D**: dry spells punctuating the wet Holocene period. See Fig. 2 for site location.

Fig. 4. Relations entre insolation et balance hydrique de quelques basins lacustres des tropiques nord et sud au cours des 25 derniers milliers d'années. **A**: Radiation solaire en été [2] ; **B** d'après [27] ; **C** d'après [15] ; **D**–**E** d'après [1]. **LGM** : Dernier maximum glaciaire ; **YD** : Dryas récent ; flèches en **C** et **D** : brefs événements arides ponctuant la période holocène humide. Voir la Fig. 2 pour la localisation des sites.

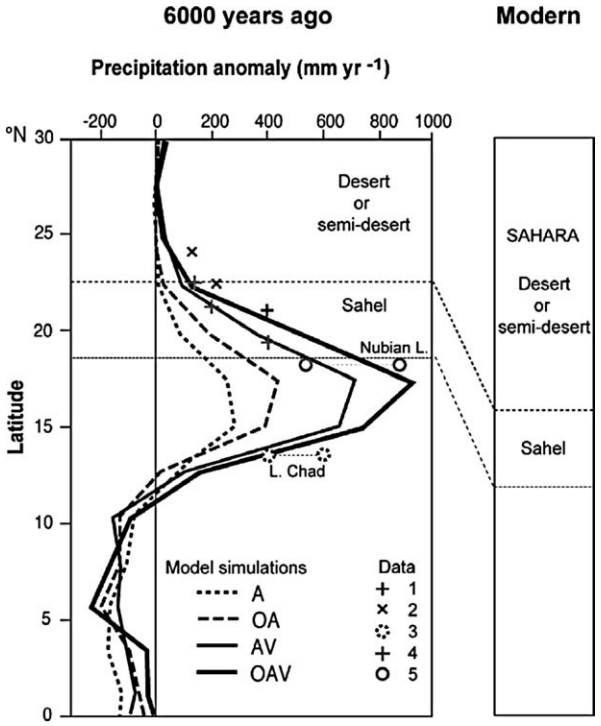

Fig. 5. Shift of the rainfall belts between the Early–Middle Holocene and the present-day [17]. Simulations of precipitation change between 6 kyr and the present-day, compared with some data-inferred precipitation changes. The four simulations curves (redrawn from [7]) derive from a series of experiments using the same model. **A**: Astronomical forcing alone; **AO**: interactive ocean; **AV**: interactive vegetation; **AOV**: ocean and vegetation. Data-inferred changes in precipitation in the Sahara–Sahel compiled in [17]. Estimated palaeoprecipitation derived from pollen records (1, after [22]) combined with numerical simulations in West Africa (2, after [28]), pollen records in eastern Sahara (4, after [24,26]), from a water-balance model of the West Nubian palaeolake [19], and a water and energy balance model of palaeolake Chad [20]. See Fig. 2 for site location.
Fig. 5. Migration des ceintures de précipitation entre l'Holocène inférieur et moyen et la période actuelle [17]. Simulations du changement de précipitation entre 6 ka et l'Actuel, comparés à quelques estimations basées sur les données géologiques. Les quatre courbes de simulation (redessinées d'après [7]) dérivent d'une série d'expériences utilisant le même modèle. **A** : Forçage astronomique seul ; **AO** : interaction avec l'océan ; **AV** : interaction avec la végétation; AOV : interaction avec l'océan et la végétation. Changements de précipitation au Sahara–Sahel, estimés à partir de données géologiques (repris de [17]). Estimations basées sur des enregistrements polliniques (1, d'après [22]) combinés à des simulations numériques (2, d'après [28]) en Afrique de l'Ouest, des enregistrements polliniques au Sahara occidental (4, d'après [24,26]), un modèle de balance hydrique du paléolac Ouest-Nubien [19] et un modèle de balance hydrique et énergétique du paléolac Tchad [20]. Voir la Fig. 2 pour la localisation des sites.

nic heat transport out of the tropics. GCMs simulate a global hydrological cycle weaker than today and a decrease in summer precipitation in most of the tropics during the LGM [8,25].

One of the most striking features of the African climate history has been the wetting of the Sahara during the EMH [15,16]. Data indicate a northward migration of tropical rainfall belts as far as 20–24°N (Fig. 5). This suggests a northward migration of the summer ITCZ and of the upper level jets which are crucial in the development of rain-bearing disturbance and of summer rainfall [16,17]. All GCMs simulations show a strengthening and a northward penetration of the African monsoon front over northern Africa at 6 ka BP, in response to increase summer insolation over the northern hemisphere and an enhanced north–south temperature gradient over the Sahara that reinforced the ocean-land pressure gradient [7,8] (Fig. 5). However, atmospheric GCMs simulations underestimated the observed northward shift; vegetation feedbacks amplify and modify the monsoon system's response to orbital forcing; in coupled ocean–atmosphere models, ocean feedbacks enhance the African monsoon, lengthen the rainfall season, and shift the belt of maximum precipitation further north ([7] and references therein). The best consistency between observations and simulations is found with coupled ocean–atmosphere–vegetation models [7,17] (Fig. 5).

5. Rapid climate changes

On timescales shorter than 1000 years, severe climatic disruptions are identified in many records [15–

18,30,31], and correspond to widespread climate events that have different regional expressions.

For example, dry spells interrupt the generally wet EMH period at ~9–8, 7–6.6, and ~6–5 ka BP in the northern tropics (Figs. 1C and 4B–C). The ~9–8-ka BP event was rapidly followed by a return to 'initial' conditions. In the African and Indian monsoon domains, it is a short, but pronounced dry interval identified in several lake, pollen and speleothem records [15, 18,23]. Summer monsoons over the Tibet Plateau, the Arabian Sea and tropical Africa weaken dramatically. In the North Atlantic, this event is a significant short-lived cooling. This interval has been generally cool over much of the northern hemisphere [23]. Several hypotheses have been proposed to explain this world-wide rapid climate change: (*i*) the outbreak of the glacial Lake Agassiz in the Laurentide at 8.2 ka BP may have abruptly slowed down the oceanic thermohaline circulation, (*ii*) increased volcanic aerosols in the northern hemisphere may have caused a cooling and a weakening of the Afro-Asian monsoon circulation; (*iii*) small fluctuations in solar output have been invoked as a contributing mechanism to Holocene monsoon variability ([23] and references therein). Whatever its causes, the ~9–8-ka-BP event reflects linkages between low- and high-latitudes climates, and associates cool poles with dry tropics, as for the glacial–interglacial variations.

Conversely, the rapid offset of the EMH wet period at ~5.5 ka BP can be regarded as a step-over shift to a new millennial-duration background climate, from relatively stable wet to dry climate at the Middle–Late Holocene boundary. Late Holocene aridity is consistent with a decrease in summer insolation, but the abruptness of the climate response to gradual insolation forcing requires strongly non-linear feedback processes. GCMs studies have invoked vegetation and ocean temperature feedbacks to explain this abrupt switch [12].

Determining the exact nature and duration of short-lived events in tropical Africa remains, however, difficult because high-resolution records are scarce, and because of the regional responses to large-scale climate events. For example, a high-resolution $\delta^{18}O$ speleothem record from the Makapansgat Valley in South Africa [30] and a similar resolution lake-level record for Lake Naivasha in Kenya [31] (Fig. 1B) are in antiphase over much of the last thousand years [30]. Presently, ENSO-induced climate variability is inversely correlated between equatorial East Africa and subtropical southern Africa [30]. The anti-correlation between the two records suggests that climate in these two regions has been paced by multidecadal–centennial shifts in the ENSO mode. The resulting latitudinal gradient of change may have been a significant factor in promoting southward migration of people from equatorial Africa when environments in the north were deteriorating and those in the south were ameliorating [30].

6. Conclusions

The past million years represent a period of profound global climate shifts well expressed in the African climate. Long-term fluctuations have been primarily paced by orbital variations of the Earth and were closely linked to the onset and amplification of the high-latitude glacial cycles. Within a glacial or interglacial period, orbital forcing alone cannot account for the magnitude of observed climate changes. The response to orbital forcing is modulated by coupled vegetation–albedo and surface ocean temperature–moisture transport feedback. Higher frequency variations can be induced by solar output variability, or by internal variations in the climate system caused by major volcanic eruptions or changes in major atmospheric circulation modes. At all timescales, climate changes in the African tropics are related to widespread, if not global, disruptions in the Earth's climate system.

References

[1] P. Barker, F. Gasse, New evidence for a reduced water balance in East Africa during the Last Glacial Maximum: implications for model-data comparisons, Quat. Sci. Rev. 22 (2003) 823–837.

[2] A. Berger, M.-F. Loutre, Insolation values for the climate of the last 10 million years, Quat. Sci. Rev. 10 (1991) 297–317.

[3] A.G.N. Bergner, M.H. Trauth, P. Blisniuk, A. Deino, M. Dühnforth, F. Gasse, M.R. Strecker, Tectonic and climatic controls of rift lakes in the Central Kenya Rift, East Africa, in preparation.

[4] R. Bobe, K. Behrensmeyer, R.E. Chapman, Faunal change, environmental variability and Late Pliocene hominid evolution, J. Hum. Evol. 42 (2002) 475–497.

[5] R. Bonnefille, Evidence for a cooler and drier climate in Ethiopian Uplands towards 2.5 Myr ago, Nature 303 (1983) 487–491.

[6] R. Bonnefille, R. Potts, F. Chalié, D. Jolly, D.O. Peyron, High-resolution vegetation and climate change associated with Pliocene *Australopithecus afarensis*, Proc. Natl Acad. Sci. USA 101 (2004) 12125–12129.

[7] P. Braconnot, S.P. Harrison, S. Joussaume, C.D. Hewitt, A. Kitoh, J.E. Kutzbach, Z. Liu, B. Otto-Bliesner, J. Syktus, N. Weber, Evaluation of PMIP coupled ocean–atmosphere simulations of the mid-Holocene, in: R.W. Battarbee, F. Gasse, C.S. Stickley (Eds.), Paleoclimate through Europe and Africa, Springer, Dordrecht, The Netherlands, 2003, pp. 515–533.

[8] P. Braconnot, S. Joussaume, N. de Noblet, G. Ramstein, Mid-Holocene and Last Glacial Maximum African monsoon changes as simulated within the Paleoclimate Modelling Intercomparison Project, Global Planet. Change 26 (2000) 51–66.

[9] T.E. Cerling, Development of grasslands, savannas in East Africa during the Neogene, Palaeogeogr. Palaeoclimatol. Palaeoecol. 97 (1992) 93–136.
[10] T.E. Cerling, R.L. Hay, An isotopic study of paleosol carbonates from Olduvai Gorge, Quat. Res. 25 (1988) 63–78.
[11] F. Chalié, F. Gasse, A 13 500 years diatom record from the tropical East African Rift Lake Abiyata (Ethiopia), Palaeogeogr. Palaeoclimatol. Palaeoecol. 187 (2002) 259–283.
[12] M. Claussen, C. Kubatzki, V. Brovkin, A. Ganopolski, P. Hoelzmann, H.-J. Pachur, Simulation of an abrupt change in Saharan vegetation in the mid-Holocene, Geophys. Res. Lett. 26 (14) (1999) 2037–2040.
[13] P.B. de Menocal, African climate change and faunal evolution during the Pliocene-Pleistocene, Earth Planet. Sci. Lett. 220 (2004) 3–24.
[14] F. Gasse, Tectonic and climate controls on lake distribution and environments in Afar from Miocene to present, in: B.J. Katz (Ed.), Lacustrine basin exploration – Case studies and modern analogs, Am. Assoc. Pet. Geol. Mem. 50, 1990, pp. 19–41.
[15] F. Gasse, F., Hydrological changes in the African tropics since the Last Glacial Maximum, Quat. Sci. Rev. 19 (2000) 189–211.
[16] F. Gasse, Diatom-inferred salinity and carbonate oxygen isotopes in Holocene waterbodies of the western Sahara and Sahel (Africa), Quat. Sci. Rev. 21 (2002) 737–767.
[17] F. Gasse, N. Roberts, Late Quaternary hydrologic changes in the arid and semi-arid belt of northern Africa. Implications for past atmospheric circulation, in: H.F. Diaz, R.S. Bradley (Eds.), The Hadley Circulation: Present, Past and Future, Springer, Dordrecht, The Netherlands, 2004.
[18] F. Gasse, E. Van Campo, Abrupt post-glacial climate events in West Asia and North Africa monsoon domains, Earth Planet. Sci. Lett. 126 (1994) 435–456.
[19] P. Hoelzmann, H.-J. Kruse, F. Rottinger, Precipitation estimates for the eastern Saharan palaeomonsoon based on a water balance model of the West Nubian palaeolake basin, Global Planet. Change 26 (2000) 105–120.
[20] J.E. Kutzbach, Estimates of past climate at Paleolake Chad, North Africa, based on a hydrological and energy balance model, Quat. Res. 14 (1980) 210–223.
[21] D. Legesse, C. Vallet-Coulomb, F. Gasse, F., Analysis of the hydrological response of a tropical terminal lake, Lake Abiyata (Main Ethiopian Rift Valley) to changes in climate and human activities, J. Hydrol. Processes 18 (2004) 487–504.
[22] A.M. Lézine, Late Quaternary vegetation and climate of the Sahel, Quat. Res. 32 (1989) 314–334.
[23] P.A. Mayewski, E.J. Rohling, J.C. Stager, W. Karlén, K.A. Maasch, L.D. Meeker, E.A. Meyerson, F. Gasse, S.V. Kreveld, K. Holmgren, J. Lee-Thorp, G. Rosqvist, F. Rack, M. Staubwasser, R.R. Schneider, E. Steig, (Castine Project Members), Holocene Climate Variability, Quat. Res. 62 (2004) 243–255.
[24] J.C. Ritchie, C.V. Haynes, Holocene vegetation zonation in the eastern Sahara, Nature 330 (1987) 645–647.
[25] S. Pinot, G. Ramstein, S.P. Harrison, I.C. Prentice, J. Guiot, M. Stute, S. Joussaume, Tropical paleoclimates at the Last Glacial Maximum: comparison of Paleoclimate Modeling Intercomparison Project (PMIP) simulations and paleodata, Clim. Dyn. 15 (1999) 857–874.
[26] J.C. Ritchie, C.H. Eyles, C.V. Haynes, Sediment and pollen evidence for an Early to mid-Holocene humid period in the eastern Sahara, Nature 314 (1985) 352–355.
[27] M. Servant, S. Servant-Vildary, L'environnement Quaternaire du bassin du Tchad, in: M.A.J. Williams, H. Faure (Eds.), The Sahara and the Nile. Quaternary environments and prehistoric occupation in northern Africa, Balkema, Rotterdam, The Netherlands, 1980, pp. 133–162.
[28] F.A. Street-Perrott, J.F.B. Mitchell, D.S. Marchand, J.S. Brunner, Milankovitch and albedo forcing of the tropical monsoons: a comparison of geological evidence and numerical simulations for 9000 yr BP, Trans. R. Soc. Edinb. 81 (1991) 407–427.
[29] M.H. Trauth, A.L. Deino, A.G.N. Bergner, M.R., A.G.N. Strecker, East Africa climate change and orbital forcing during the last 175 kyr BP, Earth Planet. Sci. Lett. 2006 (2003) 297–313.
[30] P.D. Tyson, J. Lee-Thorp, K. Holmgren, J.F. Thackeray, Changing gradients of climate change in southern Africa during the past millennium: implications for population movements, Clim. Change 52 (2002) 129–135.
[31] D. Verschuren, K.R. Laird, B.F. Cumming, Rainfall and drought in equatorial East Africa during the past 1100 years, Nature 403 (2000) 410–414.